High cycle fatigue properties of cast Mg–xNd–0.2Zn–Zr alloys

Liming Peng · Penghuai Fu · Zhenming Li ·
Yingxin Wang · Haiyan Jiang

Abstract The tensile and fatigue strength of cast Mg–xNd–0.2Zn–0.45Zr alloys ($x = 0$, 1, 2, 3 wt%) in both solution-treated (T4) and solution + 200 °C peak-aged (T6-PA) conditions were investigated in the present study. The results indicate that Neodymium (Nd) is an effective element to improve both the tensile and fatigue properties of cast Mg–0.2Zn–Zr alloys. The strengthening effect depends on its content in a way of power function ($\sigma = \sigma_0 + K\,C_{Nd}{}^{n}$), where the power exponent n is about 0.52–0.54 for yield strength (YS) and 0.59–0.61 for fatigue strength. The yield strengthening effect of Nd element in the form of precipitates (T6-PA) is about three times of that as solution atoms (T4), while the fatigue strengthening effect of Nd element in the form of precipitates is only about 50 % higher than that as solution atoms. The improved strength (both YS and ultimate tensile strength) can lead to the same amount improvement of the fatigue strength in T4-treated alloys, while only can cause less than half improvement of the fatigue strength in T6-PA-treated alloys.

L. Peng · P. Fu (✉) · Z. Li · Y. Wang · H. Jiang
National Engineering Research Center of Light Alloys Net
Forming and State Key Laboratory of Metal Matrix Composite,
Shanghai Jiao Tong University, 200030 Shanghai, People's
Republic of China
e-mail: fph112sjtu@sjtu.edu.cn

L. Peng
e-mail: plm616@sjtu.edu.cn

Z. Li
e-mail: bojin516@yahoo.com.cn

Y. Wang
e-mail: wyx119@sjtu.edu.cn

H. Jiang
e-mail: jianghy@sjtu.edu.cn

Introduction

Magnesium (Mg) alloys become very attractive because of their low density, high specific strength and easy recyclability. There is significant increase in the usage of Mg alloys in automobile, aerospace and other transportation industries [1]. Compared with their wrought counterparts, cast Mg alloys have clear economic advantages for mass production of components due to their lower long-term processing and assembly costs. Almost 90 % of total Mg alloy productions involve casting processes [2]. Lots of researches were carried out on a better understanding of the fatigue characteristics of cast Mg alloys. Most of them were focused on the influence of casting defects. The results show that cast Mg alloys always suffer easy fatigue crack initiations due to the existence of casting defects, such as gas pores or shrinkages [3–5], on or below the surface of cast components. Regarding high cycle fatigue tests, it was suggested that crack initiation takes up most of the fatigue life [6]. Therefore, those casting defects, as crack initiation, obviously deteriorated the fatigue properties of cast Mg alloys. Any innovative process, which could reduce the level of casting defects, of course, can improve the fatigue properties of cast Mg alloys. Quite a few researches focused on the individual influence of microstructure characteristics on the fatigue properties, such as the grain size, secondary compounds, precipitates, especially for cast Mg alloys, because casting defects are always the reasons of the failure. As a result, a thorough understanding of the influence of the critical microstructural features on the fatigue behaviors of cast Mg alloys is still unavailable. Due to the progress of technology, more and more sound casting components could be produced by squeeze casting, vacuum die casting and low pressure die casting processes, which make the study of microstructure-based fatigue mechanisms become necessary.

These critical microstructural features of cast Mg alloys are further determined by their chemical composition, heat treatment conditions and casting processes. The different contents of precipitations in AZ31, AZ61 and AZ91 Mg alloys, caused by the different Al additions, of course, could influence the fatigue behavior of Mg–Al alloys. Compared with as-cast condition, solution and aging treatment (T6 condition) increase the rotary bending fatigue strength of cast Mg–10Gd–3Y–Zr alloy [7], from 85 to 105 MPa. Our recent study about AM-SC1 alloy [8] indicated that, though the fatigue strength of AM-SC1 alloy solution treated at a higher temperature increases, the fatigue life under the stresses higher than fatigue strength are obviously reduced compared with the alloy solution treated at a lower temperature. Casting processes usually determine the cooling rates of the solidification, which in turn leads to different microstructure. The higher cooling rate in high pressure die casting produces finer microstructures, such as grains of 10 μm and even finer eutectics in AZ91 Mg alloy [9], while the lower cooling rate in sand casting manufactures coarser microstructures, such as grains of 70–80 μm even in a Zr-refined Mg–4Y–2Nd–1Gd alloy [10]. The finer microstructures, such as finer grains, usually can enhance the fatigue strength of Mg alloys, which is already confirmed in cast AM-SC1 [11], extruded AZ31 [12] alloys. Therefore, by influencing the critical microstructural features, the chemical composition, heat treatments and casting processes in turn can have obvious effects on the fatigue behaviors of cast Mg alloys. To facilitate the interactive microstructure-based design of cast components for long-life behavior, the fatigue mechanisms must be linked to the critical microstructural features in cast Mg alloys, not just casting defects. The relationships among the chemical composition/heat treatment conditions/casting processes, the critical microstructural features and the fatigue behaviors need to be revealed in detail.

Mg–3Nd–0.2Zn–Zr (wt%) (NZ30K) [13–15] is a newly developed magnesium alloy, which has better mechanical properties than the commercial AZ91D alloy at both room and high temperature. The main strengthening phases in NZ30K alloy are the meta-stable β'' (DO_{19} structure, $a = 0.64$ nm, $c = 0.52$ nm) and β' (face-centered cubic structure, $a = 0.736$ nm) phases [13], which precipitate at 200 °C and strengthen the alloy at both room and relatively high temperature (200–250 °C). NZ30K is very attractive for the Power-Train Application in Auto Industry, where the high temperature (150–250 °C) properties are required. As a Rare Earth (RE) containing alloy refined by Zr, the cost of NZ30K alloy is much higher than the commercial AZ91D alloy. It is quite necessary to know whether the addition of Nd content can be reduced based on the relationship between the chemical composition and the fatigue

Table 1 Chemical compositions of cast Mg–xNd–Zn–Zr alloys (wt%)

Alloys	Zr	Nd	Zn	Mg
NZ00K	0.46	0	0.19	Bal.
NZ10K	0.44	0.97	0.22	
NZ20K	0.44	1.92	0.21	
NZ30K	0.45	2.98	0.19	

performance. Therefore, in the present study, the influences of Nd variation and heat treatment on the tensile and fatigue properties of Mg–Nd–0.2Zn–Zr alloy based on gravity permanent casting were carried out.

Experimental procedure

Alloys and heat treatment

The materials used in the present work were gravity permanent mold cast plates [16]. Round bars (13 mm in diameter × 130 mm in length) for tensile/fatigue test were sectioned from the cast plates [16]. Nominal composition of Mg–xNd–0.2Zn–0.45Zr (x = 0, 1, 2, 3 wt%, all compositions in wt% except otherwise stated) (designated as NZ00K, NZ10K, NZ20K, NZ30K, respectively) alloys were prepared using high purity Mg, Zn and Mg–25Nd, Mg–30Zr master alloys in an electrical resistance furnace under the protection of a gas mixture of SF_6, CO_2 and air, and cast into a metal mold at pouring temperature of 740 ± 5 °C and mold temperature of 200 ± 5 °C. The actual chemical compositions of the alloys were measured using inductively coupled plasma (ICP) technique, and the results are listed in Table 1. The cast plates were first solution treated at 540 °C for 10 h, quenched into hot water at about 70 °C (designated as T4), then peak-aged at 200 °C for 14 h (T6-PA).

Tensile testing

Cylindrical tensile specimens with a diameter of 6 mm and a gauge length of 30 mm were tested at room temperature on a Zwick/Roell-20KN machine at a crosshead speed of 1 mm/min. Stress–strain curves were obtained by attaching a knife-edge extensometer to the gauge section. The ultimate tensile strength, yield strength and elongation of specimens were determined from the test data. The Hollomon equation ($\sigma = K\varepsilon^n$) was assumed to represent the stress–strain curves of magnesium alloys in plastic deformation stage, and the strain-hardening exponent (n value) was determined from a linear fit to the log true stress–log true strain data [17]. It should note here that as there is nearly no precipitation strengthening in Mg–0.2Zn–0.45Zr
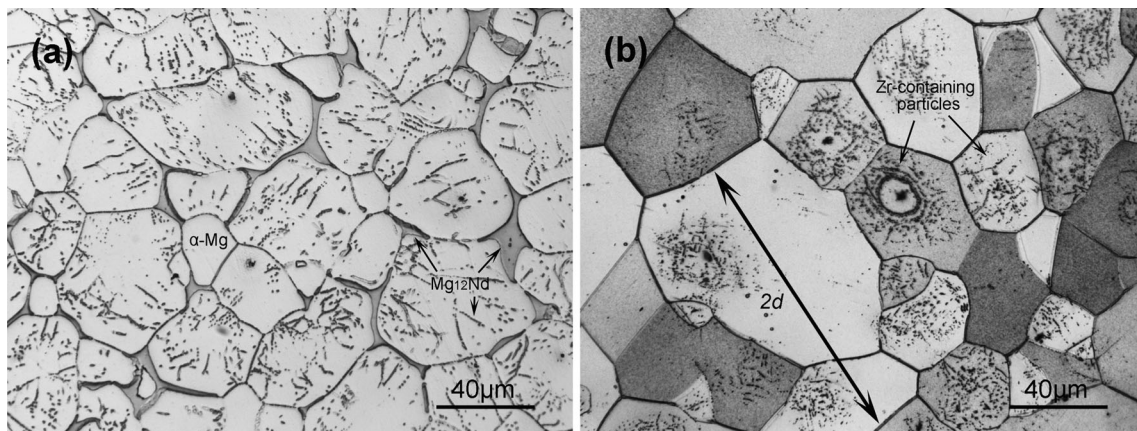
Fig. 1 Optical micrographs of cast Mg–xNd–0.2Zn–0.45Zr alloys (the average grain size is about 60 μm): **a** 3Nd, as-cast condition; **b** 3Nd, T6-PA condition. The way in which grain sizes are measured is shown in (**b**)

alloy, tensile properties of Mg–0.2Zn–0.45Zr alloy were only test in as-cast condition.

Fatigue testing

Hour-glass-shaped round specimens, with a minimum gage diameter of 6 mm according to ASTM E466 specification, were used for fatigue test. The gage surfaces of all fatigue specimens were polished using abrasive paper of grit 1600 and then buff-polished to avoid the influence of machining on the fatigue results. Fatigue test was performed under rotary beam loading ($R = -1$) at a frequency of 100 Hz in air (temperature 25–35 °C), with relative humidity of 40–60 %. The load-controlled staircase (SC) fatigue test was adopted to estimate the mean and standard deviation of fatigue strength at a given number (10^7) of cycles-to-failure. The detailed method of fatigue test was given in Ref. [18], and 5 MPa was chosen as step size. Fatigue properties of Mg–0.2Zn–0.45Zr alloy were test only in as-cast condition.

Microstructural analysis

Samples for microstructural analysis were obtained from the cross sections of the clamping areas of the tensile specimens and were etched in a solution of 12 g picric acid + 80 ml acetic acid + 80 ml water + 350 ml ethanol. Zeiss Observer optical microscopy (OM) was used to observe the morphology and distribution of the various phases present. The average grain size (d) of the alloys was calculated from the optical micrographs using a linear intercept method ($d =$ the linear intercept size, as shown in Fig. 1b) on at least 400 grains. Fracture surfaces of the tensile specimens were investigated in a JEOL JSM-6460 scanning electron microscope (SEM).
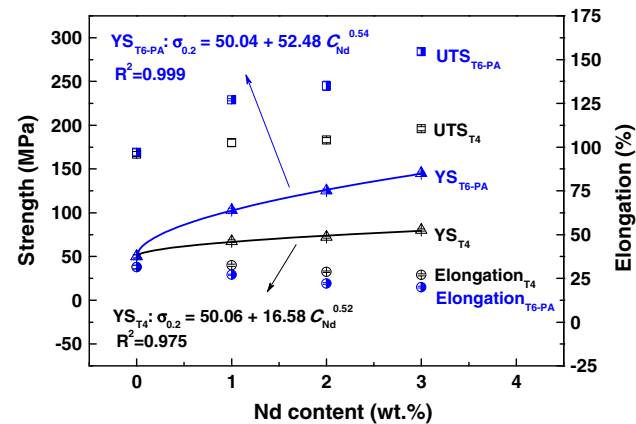
Results

Microstructure

Figure 1 shows the typical microstructure of cast Mg–xNd–0.2Zn–0.45Zr alloys ($x = 3$ wt%). As stated in previous studies [13, 14], the microstructure of cast Mg–3.0Nd–0.2Zn–0.45Zr alloy varies with heat treatment conditions. In as-cast condition (Fig. 1a), it contains α-Mg matrix and $Mg_{12}Nd$ eutectic compounds. Through solution treatment (T4), the $Mg_{12}Nd$ compounds dissolve into the α-Mg matrix to form supersaturated solid solution (Nd element exists as solution atoms), meanwhile fine Zr-containing particles (indicated in Fig. 1b) [19–21] precipitate at grain interiors. The distribution of these precipitates is governed predominantly by the coring of the Zr content during solidification which is associated with the grain refining process [20]. Following peak aging treatment (T6-PA) does not influence the composition and distribution of Zr-containing particles, but let the supersaturated solid solution decompose into meta-stable precipitates of β″ phases with DO_{19} structure and α-Mg matrix [13, 22]. The β″ precipitates are the main strengthening phases in T6-PA alloys. The constitutions of the alloys in different thermal conditions are summarized in Table 2. It should mention that, since Mg–0.2Zn–0.45Zr alloy only consists of α-Mg matrix with little solution (0.2 wt% Zn), it has no aging hardening ability. Only as-cast Mg–0.2Zn–0.45Zr alloy was studied as base alloy. The main differences of different Nd addition alloys are the content of $Mg_{12}Nd$ eutectic compounds in as-cast condition, solution atoms (Nd) in T4 condition and β″ phases in T6-PA condition. The more Nd additions, the higher content of $Mg_{12}Nd$ eutectic compounds in as-cast condition, solution atoms (Nd) in T4 condition and β″ phases in T6-PA condition. The different content of

Table 2 Phase constitutions of cast Mg–xNd–Zn–Zr alloys in different thermal conditions

Alloy	As-cast	T4	T6
NZ00K	α-Mg	–	–
NZ10K	α-Mg + Mg$_{12}$Nd compounds	α-Mg (S.S.S.S.) + Zr-containing particles	α-Mg + Zr-containing particles + β'' precipitates
NZ20K	α-Mg + Mg$_{12}$Nd compounds	α-Mg (S.S.S.S.) + Zr-containing particles	α-Mg + Zr-containing particles + β'' precipitates
NZ30K	α-Mg + Mg$_{12}$Nd compounds	α-Mg (S.S.S.S.) + Zr-containing particles	α-Mg + Zr-containing particles + β'' precipitates

S.S.S.S. Supersaturated Solid Solution

Table 3 Tensile properties of cast Mg–xNd–Zn–Zr alloys

Alloy	YS-$\sigma_{0.2}$ (MPa)	UTS-σ_b (MPa)	Elongation (%)
NZ00K	50.0 ± 3.4	167.0 ± 3.0	20.0 ± 2.0
NZ10K			
T4	67.5 ± 3.3	180.0 ± 4.1	21.1 ± 1.1
T6	103.0 ± 1.6	229.3 ± 1.3	10.9 ± 1.6
NZ20K			
T4	72.2 ± 3.0	181.0 ± 2.9	18.6 ± 0.8
T6	125.3 ± 2.1	245.1 ± 5.3	9.0 ± 0.9
NZ30K			
T4	80.2 ± 3.0	196.0 ± 2.3	16.2 ± 0.3
T6	145.1 ± 3.0	284.3 ± 3.5	5.1 ± 0.5

Fig. 2 Tensile properties of cast Mg–xNd–0.2Zn–0.45Zr alloys as a function of Nd content, in both T4 and T6-PA conditions. *Error bars* show the standard deviation for four samples in each condition

Fig. 3 True stress–true plastic strain curves of cast Mg–xNd–0.2Zn–0.45Zr alloys, in both T4 and T6-PA conditions
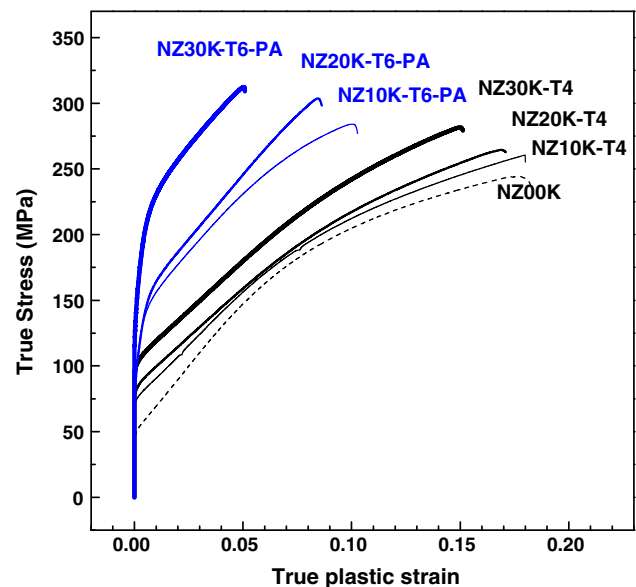
solution atoms (Nd) in T4 condition and β'' phases in T6-PA condition lead to different tensile and fatigue properties, which will be discussed later. Since the chemical compositions of Zn and Zr elements are in the same level (Table 1), the influence of Zr-containing particles in different Nd addition alloys could be considered the same. The average grain size of Mg–xNd–0.2Zn–0.45Zr alloys is not significantly affected by the Nd content and thermal conditions. In the present study, 0.45 wt% Zr is corresponding to the average grain size of about 60 μm.

Tensile properties

The tensile properties of both T4-treated and T6-PA-treated Mg–xNd–0.2Zn–0.45Zr alloys are plotted in Fig. 2 and details are list in Table 3. These results show that both the yield strength (YS) and the ultimate tensile strength (UTS) of Mg–xNd–0.2Zn–0.45Zr alloys in both T4 and T6-PA

conditions increase with the Nd content. With the best fit of the testing data in Fig. 2, there are good correlations between the YS ($\sigma_{0.2}$) and the Nd content (C_{Nd}, wt%) and can be expressed in a power function ($\sigma_{0.2} = \sigma_0 + K C_{Nd}{}^n$) as:

$$\sigma_{0.2} \approx 50.06 + 6.58 C_{Nd}^{0.52}, \text{in T4 condition} \tag{1}$$

$$\sigma_{0.2} \approx 50.04 + 52.48 C_{Nd}^{0.54}, \text{in T6 – PA condition} \tag{2}$$

The YS increases with the Nd content in both T4 and T6-PA conditions in a way of power function. The strengthening rate of Nd addition in T6-PA-treated alloys is 52.48 [MPa/(wt%)$^{0.54}$] (Eq.(2)), which is much higher than 16.58 [MPa/(wt%)$^{0.52}$] (Eq.(1)) in T4-treated alloys. Since the strengthening exponents of T4 (0.52) and T6 (0.54) conditions are very close, the strengthening effect in the form of precipitates (T6) is much higher than that in the form of solution atoms (T4). On the other hand, the ductility of
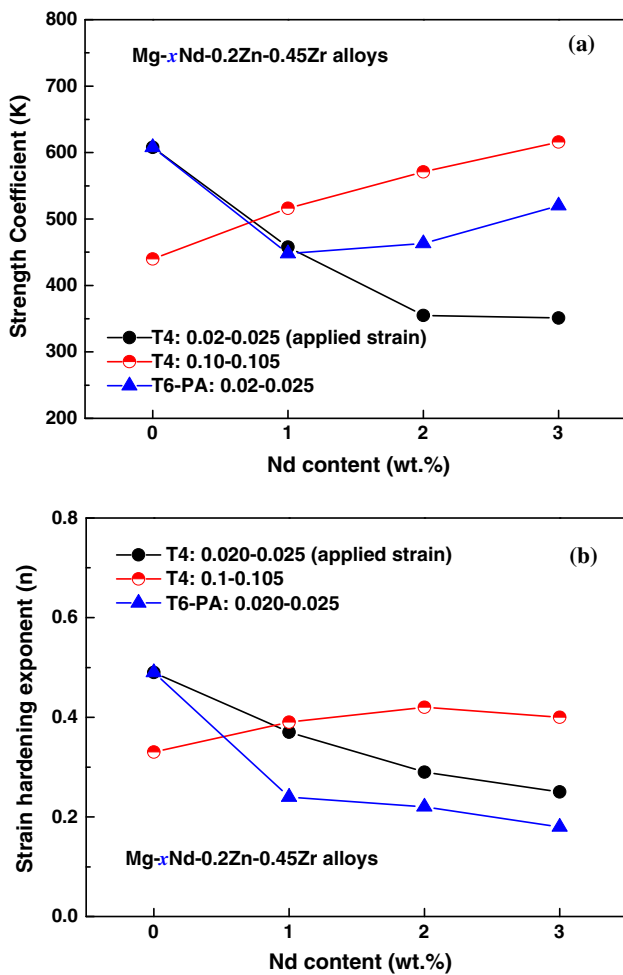
Fig. 4 Strength coefficient (**a**) and (**b**) strain-hardening exponent of Mg–xNd–0.2Zn–0.45Zr alloys as a function of Nd content, in both T4 and T6-PA conditions

alloys decreases with the Nd content (Fig. 2 and Table 3). Such reduction is much obvious for 3Nd containing alloy (NZ30K) in T6-PA condition, whose elongation is only 5.1 %, compared with 10.9 and 9.0 % of 1Nd (NZ10K) and 2Nd (NZ20K) containing alloys.

Strain-hardening behavior

Figure 3 shows the influence of Nd content on the flow behavior of cast Mg–xNd–0.2Zn–0.45Zr alloys in both T4 and T6-PA conditions. Generally, the T4-treated alloys have higher ductility, while the T6-PA-treated alloys get higher YS. With the increase of Nd content, the YS (where to start the plastic deformation, strain <1 %) obviously increases in both T4 and T6-PA-treated alloys, and more obviously in T6-PA-treated alloys.

Figure 4a illustrates the influence of Nd content on the strength coefficient ($d\sigma/d\varepsilon^n$, calculated from Hollomon equation $\sigma = K\varepsilon^n$) at plastic strains from 0.02 to 0.025 and
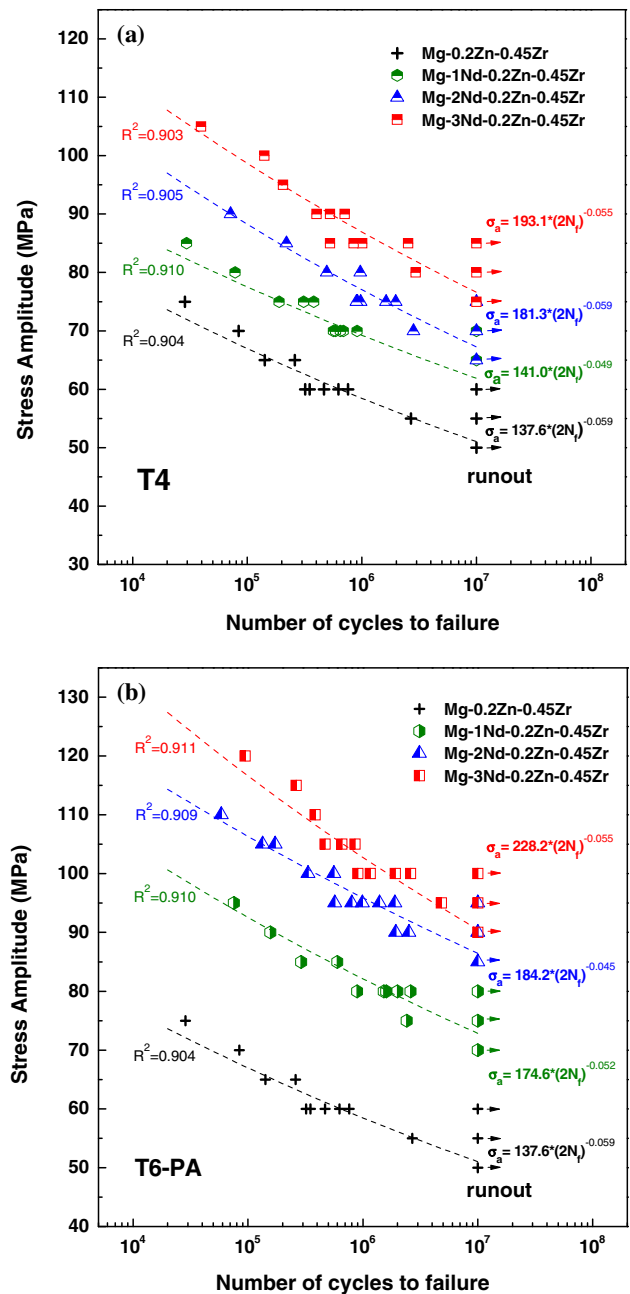

Fig. 5 S–N curves of cast Mg–xNd–0.2Zn–0.45Zr alloys: **a** T4 condition and **b** T6-PA condition

from 0.10 to 0.105, in T4-treated alloys, and from 0.02 to 0.025 in T6-treated alloys. For alloys in T4 condition, the increase of the Nd content significantly reduces the strength coefficient at the lower strains (0.02–0.025). While at the larger strains (0.10–0.105), however, the increase of the Nd content enhances the strength coefficient. It shows that the more concentrated alloys exhibit the more strain hardening at larger strains. For the alloys in T6-PA condition, at the strain range of 0.02–0.025, the increase of the Nd content from 0 to 1 wt% leads to the drop of strength

Table 4 Fatigue properties of cast Mg–xNd–Zn–Zr alloys

Alloy	Fatigue strength (MPa)	$\sigma_f/\sigma_{0.2}$	σ_f/σ_b
NZ00K	55 ± 3.5	1.10	0.33
NZ10K			
T4	71 ± 2.1	1.05	0.39
T6	78 ± 3.1	0.76	0.34
NZ20K			
T4	73 ± 4.0	1.01	0.40
T6	87 ± 3.8	0.70	0.36
NZ30K			
T4	85 ± 1.5	1.06	0.43
T6	98 ± 3.5	0.68	0.35
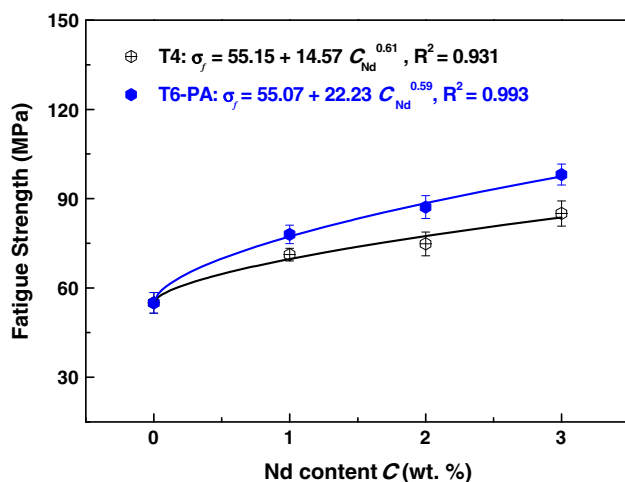
Fig. 6 Fatigue strength of cast Mg–xNd–0.2Zn–0.45Zr alloy as a function of Nd content, in both T4 and T6-PA conditions

coefficient, while the further increase of the Nd content slightly improves the strength coefficient (Fig. 4a).

Figure 4b shows the influence of Nd content on the strain-hardening exponent (n) in both T4 and T6-PA-treated alloys. For the alloys in T4 condition, the increase of the Nd content reduces the strain-hardening exponent (n) at the lower strains (0.02–0.025). While at the larger strains (0.10–0.105), however, the increase of Nd content slightly enhances the strain-hardening exponent (n) form 0 to 2 %. When further increase the Nd content to 3 %, the strain-hardening exponent (n) drops a little. For the alloys in T6-PA condition, at the strain range of 0.02–0.025, the strain-hardening exponent (n) decreases with the Nd content, a little more seriously compared with the tendency in T4 condition.

Fatigue properties

The fatigue results of cast Mg–xNd–0.2Zn–0.45Zr alloys in both T4 and T6-PA conditions are shown in Fig. 5. The fatigue strength (σ_f) and the ratios of fatigue strength to YS

and UTS of these alloys are summarized in Table 4. The fatigue properties of cast Mg–xNd–0.2Zn–0.45Zr alloys increase with the Nd content in both T4 and T6-PA conditions, and more obvious in T6-PA condition (Fig. 5b). For T4-treated alloys, the fatigue strength varies from 55 to 85 MPa. After aging, these values change from 55 to 98 MPa. The dependence of fatigue strength (σ_f) on Nd content (C_{Nd}, wt%) can be described by $\sigma_f = \sigma_0 + K\,C_{Nd}^{\,n}$, where K is the fatigue strengthening ratio, n is the fatigue strengthening exponent. With the best fit of the testing data in Fig. 6, the relationship between fatigue strength and Nd content can be expressed as:

$$\sigma_f(\text{T4}) \approx 55.15 + 14.57 C_{Nd}^{0.61}, \text{ in T4 condition} \quad (3)$$

$$\sigma_f(\text{T6}) \approx 55.07 + 22.23 C_{Nd}^{0.59}, \text{ in T6} - \text{PA condition} \quad (4)$$

The fatigue strengthening ratio in T6-PA condition (22.23, MPa/(wt%)$^{0.59}$) is higher than that in T4 condition (14.57, MPa/(wt%)$^{0.61}$). Since the fatigue strengthening exponents of T4 (0.61) and T6 (0.59) conditions are very close, the fatigue strengthening effect of Nd element as precipitates (T6-PA) is about 50 % [(22.23 − 14.57)/14.57 = 52.6 %] higher than that as solution atoms (T4). The specimens with the highest Nd content (3.0 wt%) exhibited the highest fatigue strength: 85 MPa in T4 condition and 98 MPa in T6-PA condition, respectively, which increase by 55 % (T4) and 78 % (T6-PA) compared with the Mg–0.2Zn–0.45Zr alloy.

The relationship between stress and fatigue life of Mg–xNd–0.2Zn–Zr alloy can be expressed as Basquin equation [23]: $\Delta\sigma/2 = \sigma_f'\,(2N_f)^b$, where $\Delta\sigma$ is the stress amplitude range, N_f is the fatigue life, σ_f' is the fatigue strength coefficient and b is the fatigue exponent. The fitting results are included in Fig. 5, with the average error of about 6.3 %. It can be seen that the fatigue strength coefficient σ_f' for both T4- and T6-treated alloys also increases with the Nd content. Aging treatment leads to a significant improvement of the fatigue strength coefficient σ_f' (Fig. 5) from 137.6–193.1 MPa in T4 condition to 137.6–228.2 MPa in T6 condition.

Fatigue crack initiation

The fatigue fracture surfaces of cast Mg–xNd–0.2Zn–0.45Zr alloys were carefully observed. Since the surface experiences the maximum stress during rotary beam loading, the fatigue cracks all initiate from the free surface of the fatigue samples, as indicated in Fig. 7b. Similar to AM-SC1 Mg alloy [8], the fatigue initiation regions are also falcate shaped and along the surface of the fatigue samples. However, their morphologies are different between T4- and T6-treated alloys, as indicated in Fig. 7a, b. In T4-treated alloy, there are lots of twinning-like steps distributed in the fatigue crack initiation region and the morphologies are
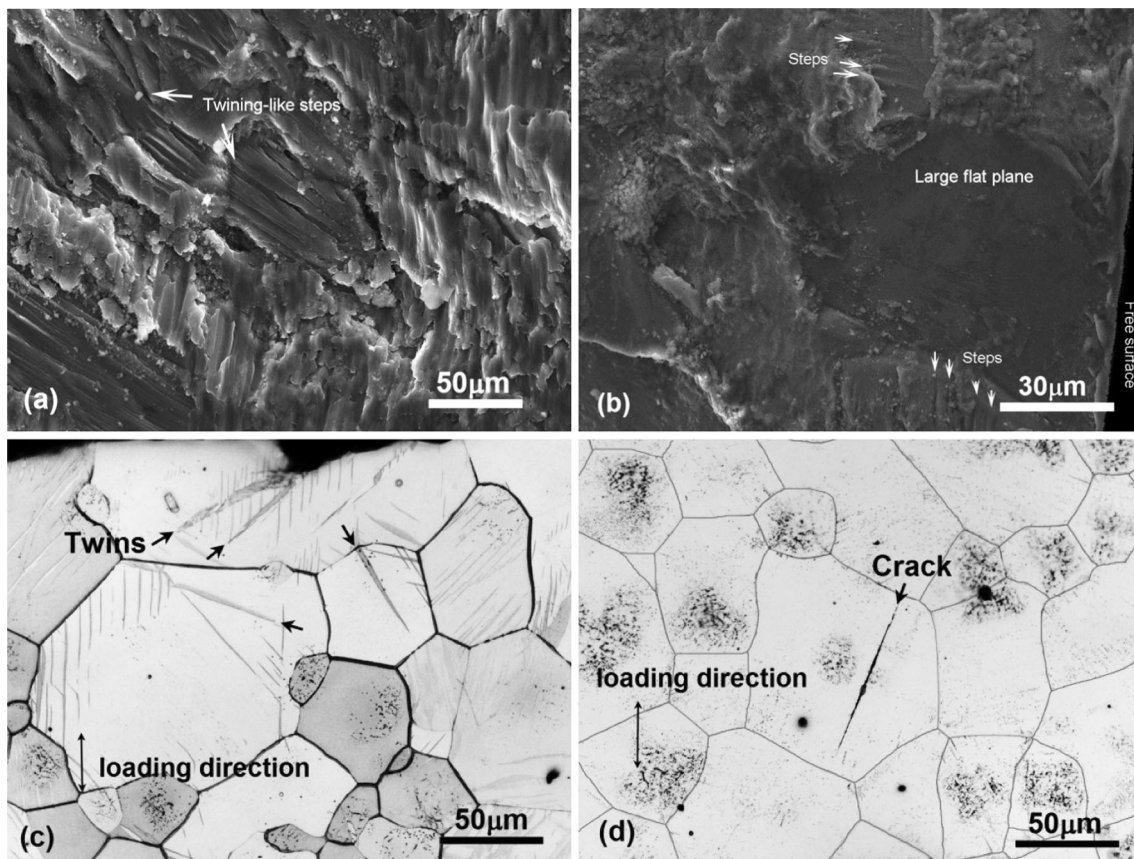
Fig. 7 SEM micrograph of fatigue crack initiation regions in cast Mg–2.0Nd–0.2Zn–0.45Zr (NZ20K) alloys: **a** T4, failed after 6.5E5 cycles at 75 MPa; **b** T6-PA, failed after 5.7E5 cycles at 95 MPa.

Optical image of the specimens section parallel to the gage length beneath the fatigue crack initiation regions: **c** T4 and **d** T6-PA

more obvious (Fig. 7a). While in T6-treated alloy, a large flat plane of grain size large is observed, as shown in Fig. 7b. There are also some fine steps around the large flat plane. However, the total amount of steps-like morphologies is much less in T6-treated alloy than those in T4-treated alloy. The microstructures below the crack initiation area of cast Mg–xNd–0.2Zn–Zr alloys are shown in Fig. 7c, d. There are lots of twinning in T4-treated alloys, while it is hardly observed in T6-treated alloys. The morphology of secondary fatigue crack look like a straight line in T6-treated alloy, which is more likely to initiate from the slip lines [24, 25]. Compared the fracture surface in Fig. 7a, c with the microstructure in Fig. 7b, d, it seems that twinning plays more important roles in T4-treated alloys than that in T6-treated alloys.

Discussion

Strengthening mechanism of Nd addition

In cast Mg alloys, the strengthening mechanisms usually include pure Mg (σ_{Mg}), secondary phase strengthening (σ_{sp}), solid solution strengthening (σ_{ss}), precipitation strengthening (σ_{ppt}) and grain boundary strengthening (σ_{gb}). Compared with as-cast alloys (Fig. 1a), the eutectics along the grain boundaries all dissolve into the matrix during solution treatment [13, 14]. Only the fine Zr-containing particles [19] precipitate at grain interiors (Fig. 1b). The influence of these particles on mechanical properties is unclear. They are unlikely to provide a significant contribution to the overall mechanical properties of the alloy due to their large size and less in density [20]. Therefore, their influence on the yield and fatigue strength is ignored here. Considering in this way, in T4-treated Mg–xNd–0.2Zn–0.45Zr alloys, besides the pure Mg (σ_{Mg}) and grain boundary strengthening (σ_{gb}), only solid solution strengthening (σ_{ss}) contributes to the YS. After aging treatment, most of Nd element precipitates in the form of meta-stable phases (mainly the β'' phases with DO_{19} structure [13, 22]). As the solid solubility of Nd element at 200 °C is only about 0.08 %, the solid solution strengthening effect in aged Mg–xNd–0.2Zn–0.45Zr alloy could be ignored. Therefore, in T6-treated alloys, besides the pure Mg (σ_{Mg}) and grain boundary strengthening (σ_{gb}), only precipitation strengthening (σ_{ppt}) contributes to the YS.

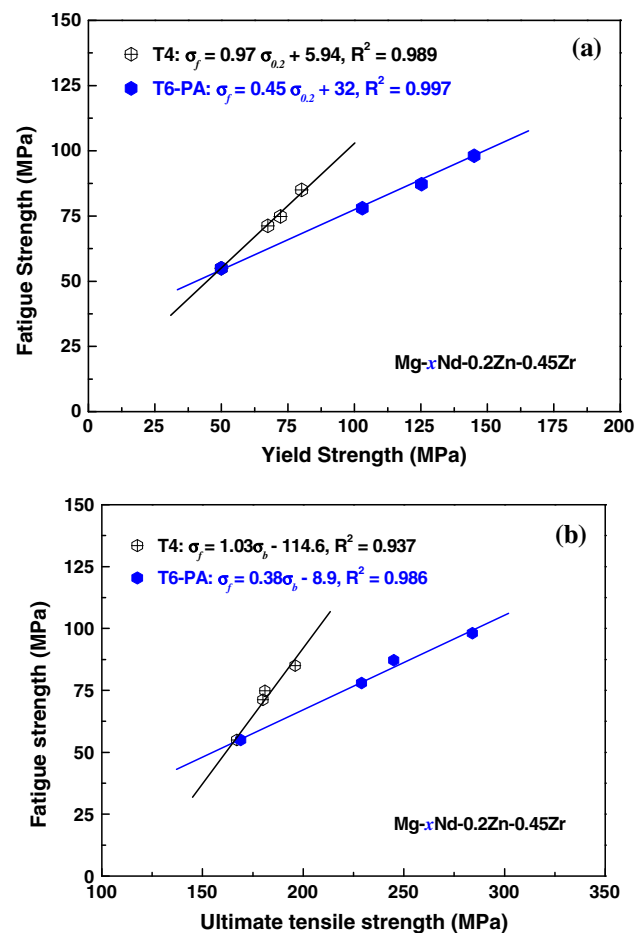**Table 5** Strengthening contribution to the yield strength in cast Mg–xNd–Zn–Zr alloys

Alloy	Solid solution strengthening (σ_{ss})		Precipitation strengthening (σ_{ppt})		Yield strength	σ_{ppt}/σ_{ss}
	MPa	%	MPa	%		
NZ00K	–	–	–	–	50.0	–
NZ10K						
T4	17.5	26	–	–	67.5	3.0
T6-PA	–	–	53.0	51	103.0	
NZ20K						
T4	22.2	31	–	–	72.2	3.4
T6-PA	–	–	75.3	60	125.3	
NZ30K						
T4	30.2	38	–	–	80.2	3.1
T6-PA	–	–	95.1	65	145.1	

Table 6 Strengthening contribution to the fatigue strength in cast Mg–xNd–Zn–Zr alloys

Alloy	Solid solution strengthening (σ_{ss})		Precipitation strengthening (σ_{ppt})		Fatigue strength	σ_{ppt}/σ_{ss}
	MPa	%	MPa	%		
NZ00K	–	–	–	–	55	–
NZ10K						
T4	16	22.5	–	–	71	1.44
T6-PA	–	–	23	29.5	78	
NZ20K						
T4	18	24.7	–	–	73	1.78
T6-PA	–	–	32	36.8	87	
NZ30K						
T4	30	35.3	–	–	85	1.43
T6-PA	–	–	43	43.9	98	

The YS of Mg–0.2Zn–0.45Zr alloy without Nd addition is 50 MPa (Table 3). The solution strengthening contribution in T4-treated alloy and the precipitation strengthening contribution in T6-treated alloy coming from Nd additions could be estimated as (YS–50) MPa. Calculation in this way, the strengthening contributions to the YS in both T4- and T6-treated alloys can be summarized in Table 5. The strengthening contributions to the YS of 1Nd, 2Nd and 3Nd addition are 17.5, 22.2, 30.2 MPa in the form of solid solution (solution atoms), and 53, 75, 95 MPa in the form of precipitation (precipitates). The strengthening effect in the form of precipitates is about three times of that in the form of solution atoms. The ratios of σ_{ppt}/σ_{ss} in 1Nd, 2Nd and 3Nd containing alloys are 3.0, 3.4, 3.1 (Table 5), respectively.

If similar consideration was applied to the fatigue strength, the strengthening contributions to the fatigue strength in both T4- and T6-treated alloys can also be obtained in Table 6. The strengthening contributions to the fatigue strength of 1Nd, 2Nd and 3Nd addition are 16, 18, 30 MPa in the form of solution atoms, and 23, 32, 43 MPa in the form of precipitates. The strengthening effect in the form of precipitates is only about 1.43–1.78 times of that in the form of solution atoms. The ratios of σ_{ppt}/σ_{ss} in 1Nd, 2Nd and 3Nd containing alloys are 1.44, 1.78, 1.43 (Table 6), respectively. Compared with the contributions to the YS (Table 5), the ratios of σ_{ppt}/σ_{ss} decrease from about 3 in YS to 1.43–1.78 in fatigue strength, and the difference of the contributions to the fatigue strength between the solution atoms and the precipitates obviously reduces. If the absolute value was considered, the contribution coming from the precipitates is still much higher (43–78 %) than that of solution atoms in the case of fatigue strength.

Fig. 8 The relationship between the yield strength (**a**), ultimate tensile strength (**b**) and fatigue strength of cast Mg–xNd–0.2Zn–0.45Zr alloys, in both T4 and T6-PA conditions

The relationship between fatigue strength and tensile properties

The relationship between the YS, UTS and fatigue strength of cast Mg–xNd–0.2Zn–0.45Zr alloys in both T4 and T6-PA conditions are shown in Fig. 8. There are good linear correlations between the YS ($\sigma_{0.2}$) and fatigue strength (σ_f) in both T4 and T6 conditions, as shown in Fig. 8a. With the best fit of the testing data, the relationship between the fatigue strength and the YS can be expressed as:

$$\sigma_f(T4) \approx 0.97\sigma_{0.2} + 5.94, \text{in T4 condition} \quad (5)$$

$$\sigma_f(T6) \approx 0.45\sigma_{0.2} + 32, \text{in T6} - \text{PA condition} \quad (6)$$

From Eq.(5), in T4-treated Mg–xNd–0.2Zn–0.45Zr alloys, the strengthening ratio of YS ($\sigma_{0.2}$) to fatigue strength (σ_f) is as high as 0.97, much higher than that of T6-PA-treated alloy [0.45, Eq.(6)]. If the relationships of the UTS (σ_b) and the fatigue strength (σ_f) of cast Mg–xNd–0.2Zn–0.45Zr alloys were considered, good linear correlations could also be obtained in Fig. 8b and expressed as:

$$\sigma_f(T4) \approx 1.03\sigma_b - 114.6, \text{in T4 condition} \quad (7)$$

$$\sigma_f(T6) \approx 0.38\sigma_b - 8.9, \text{in T6} - \text{PA condition} \quad (8)$$

Similar to Eq.(5) and Eq.(6), the strengthening ratio of UTS (σ_b) to fatigue strength (σ_f) in T4-treated alloys (1.03) is obviously higher than that of T6-PA-treated alloy (0.38). It seems that the strength improvement (both YS and UTS) can lead to the same amount improvement in the fatigue strength in T4-treated Mg–xNd–0.2Zn–0.45Zr alloys, while only can give less than half improvement in the fatigue strength in T6-PA-treated alloys.

These significant differences of the strengthening ratios of YS and UTS to fatigue strength in different thermal conditions may come from the different deformation mechanisms during fatigue tests, as shown in Fig. 7. As described above, in T4-treated Mg–xNd–0.2Zn–0.45Zr alloys, lots of twinnings are observed beneath the fatigue fracture surface (Fig. 7c), while it is very hard to find in T6-PA-treated alloys (Fig. 7d). The tendency of twinning formation seems to have a very close relationship with the existing form of strengthening elements (Nd in the present alloys). In T4-treated condition, Nd element exists as solution atoms. Though such existence can strengthen the alloy, but in a lower efficiency, as indicated in Eq.(1), the strengthening ratio is only 16.58 [MPa/(wt%)$^{0.52}$], which is much lower than the strengthening ratio as precipitates in T6-PA-treated alloy [52.48 (MPa/(wt%)$^{0.54}$), Eq.(2)]. In T4-treated alloy, with lower YS (67.5–80.2, Table 3), twinning is easily activated during deformation, both in tensile and fatigue tests (Fig. 7c). While in T6-PA-treated alloy, with higher YS (103.0–145.1, Table 3), twinning is hard to grow, both in tensile and fatigue tests (Fig. 7d),

which is also confirmed in the literature that the precipitates have strong suppression effect to the growth of twinning [26]. Therefore, probably, the different deformation mechanisms in T4 and T6-PA-treated alloys lead to the different strengthening ratios of tensile strength (both YS and UTS) to fatigue strength. In T4-treated alloy, twinning is probably the main deformation mechanism, and the strengthening ratio of tensile strength to fatigue strength is higher [0.97 in Eq.(5) and 1.03 in Eq.(7)]. While in T6-PA-treated alloy, slip is probably the main deformation mechanism and the strengthening ratio of tensile strength to fatigue strength is lower [0.46 in Eq.(6) and 0.38 in Eq.(8)].

In the literature, the influence of alloy content and heat treatment on the fatigue strength of cast Mg alloys were seldom studied, as they always contains casting defects, which seriously reduce the fatigue properties of cast Mg alloys and make those influence much less visible. Only a few studies about the influence of heat treatment are valuable as reference. In sand cast AZ91C alloy [27], the fatigue strength of as-cast, T4-treated (solution treatment only) and T6-treated (solution + aging) conditions at 10E7 under rotary beam loading are 95, 105 and 95 MPa, respectively. Different from the present study, the subsequent aging after solution treatment leads to the drop of the fatigue strength in AZ91C alloy from 105 to 95 MPa. In wrought AZ80 Mg alloy [28], it was also reported that the fatigue strength of T5-treated (aging after extrusion) alloy is lower than that of as-extruded alloy under high cycle fatigue tests, even though higher tensile properties are got in T5-treated condition. While in hot extruded ZK60 alloy (Mg–Zn-based alloy) [29], it was found that the subsequent aging after hot extrusion (T5) enhances the fatigue strength of ZK60 alloy from 140 MPa (as-extruded) to 150 MPa (T5). Therefore, the influence of aging on the fatigue strength in Mg–Al alloys and the present Mg–xNd–0.2Zn–0.45Zr alloys (also Mg–Zn-based alloys) are different. In present cast Mg–xNd–0.2Zn–0.45Zr alloys and ZK60 alloy [29], the subsequent aging after solution treatment leads to the increase of both tensile strength and fatigue strength. However, in aging harden-able Mg–Al alloys (AZ91C [27] and AZ80 [28]), the aging treatment only improves the tensile strength while drops the fatigue strength. Those differences may come from the different types of precipitates in Mg–RE and Mg–Zn alloys and Mg–Al alloys. In Mg–RE and Mg–Zn alloys, the mainly strengthening phases are fine meta-stable precipitates (such as the β'' phase with DO$_{19}$ structure in Mg–3Nd–0.2Zn–Zr alloy [13] and the β_1' and β_2' phases in Mg–Zn-based alloy [30]) and coherent to the matrix, which could easily be cut by dislocations and lead to uniform plastic deformation. Hence, the fatigue cracks are hard to initiate and the fine precipitates improve the fatigue strength. On the contrast,

in aging harden-able Mg–Al alloys, the precipitates are large stable phases (such as large discontinuous $Mg_{17}Al_{12}$ phases along the grain boundaries in Mg–9Al alloy) and incoherent to the matrix, which are difficult to cut by dislocations. Therefore, the large stable phases easily cause high localized stress concentrations and promote the initiation of fatigue cracks. Thus, the precipitates in Mg–Al alloys (especially the discontinuous $Mg_{17}Al_{12}$ phases) reduce the fatigue strength. The detailed influences of these two kinds of precipitates on fatigue behaviors need further detail studies.

Conclusions

The tensile and fatigue strength of cast Mg–xNd–0.2Zn–0.45Zr alloys ($x = 0, 1, 2, 3$ wt%) in both solution-treated (T4) and solution + 200 °C peak-aged (T6-PA) conditions were investigated in the present study. The results indicate that Neodymium (Nd) is an effective element to improve both the tensile and fatigue properties of cast Mg–0.2Zn–Zr alloys. The strengthening effect depends on its content in a way of power function ($\sigma = \sigma_0 + K\,C_{Nd}{}^n$), where the power exponent n are about 0.52–0.54 for yield strength and 0.59–0.61 for fatigue strength. The yield strengthening effect of Nd element in the form of precipitates (T6-PA) is about three times of that as solution atoms (T4), while the fatigue strengthening effect of Nd element in the form of precipitates is only about 50 % higher than that as solution atoms. The improved strength (both yield strength and ultimate tensile strength) can lead to the same amount improvement of the fatigue strength in T4-treated alloys, while only can cause less than half improvement of the fatigue strength in T6-PA-treated alloys.

References

1. Agnew SR, Nie JF (2010) Preface to the viewpoint set on: the current state of magnesium alloy science and technology. Scripta Mater 63:671–673
2. Sajuri ZB, Miyashita Y, Hosokai Y, Mutoh Y (2006) Effects of Mn content and texture on fatigue properties of as-cast and extruded AZ61 magnesium alloys. Int J Mech Sci 48:198–209
3. Lu Y, Taheri F, Gharghouri MA, Hand HP (2009) Experimental and numerical study of the effects of porosity on fatigue crack initiation of HPDC magnesium AM60B alloy. J Alloys Compd 470:202–213
4. Horstemeyer MF, Yang N, Gall K, McDowell DL, Fan J, Gullett PM (2004) High cycle fatigue of a die cast AZ91E-T4 magnesium alloy. Acta Mater 52:1327–1336

5. Xu DK, Liu L, Xu YB, Han EH (2008) The fatigue behavior of I-phase containing as-cast Mg–Zn–Y–Zr alloy. Acta Mater 56:985–994
6. Chapetti MD, Tagawa T, Miyata T (2003) Ultra-long cycle fatigue of high-strength carbon steels part II: estimation of fatigue limit for failure from internal inclusions. Mater Sci Eng A 356:236–244
7. Liu WC, Dong J, Zhang P, Korsunsky AM, Song X, Ding WJ (2011) Improvement of fatigue properties by shot peening for Mg–10Gd–3Y alloys under different conditions. Mater Sci Eng A 528:5935–5944
8. Li ZM, Fu PH, Peng LM, Becker EP, Wu GH (2013) Influence of solution temperature on fatigue behavior of AM-SC1 cast magnesium alloy. Mater Sci Eng, A 565:250–257
9. Cáceres CH, Poole WJ, Bowles AL, Davidson CJ (2005) Section thickness, macrohardness and yield strength in high-pressure diecast magnesium alloy AZ91. Mater Sci Eng A 402:269–277
10. Liu ZJ, Wu GH, Liu WC, Pang S, Ding WJ (2012) Effect of heat treatment on microstructures and mechanical properties of sand-cast Mg–4Y–2Nd–1Gd–0.4Zr magnesium alloy. T Nonferr Metal Soc 22:1540–1548
11. Dunlop G, Bettles CJ, Griffiths JR et al (2003) The effect of grain size on the bolt load retention behaviours of AMC-SC1. In: Kainer KU (ed) The 6th International Conference Magnesium Alloys and Their Applications. Wolfsburg, Germany, pp 100–105
12. Uematsu Y, Tokaji K, Kamakura M, Uchida K, Shibata H, Bekku N (2006) Effect of extrusion conditions on grain refinement and fatigue behaviour in magnesium alloys. Mater Sci Eng A 434:131–140
13. Fu PH, Peng LM, Jiang HY, Chang JW, Zhai CQ (2008) Effects of heat treatments on the microstructures and mechanical properties of Mg–3Nd–0.2Zn–0.4Zr (wt%) alloy. Mater Sci Eng A 486:183–192
14. Fu PH, Peng LM, Jiang HY, Ma L, Zhai CQ (2008) Chemical composition optimization of gravity cast Mg–yNd–xZn–Zr alloy. Mater Sci Eng A 496:177–188
15. Li ZM, Fu PH, Peng LM, Wang YX, Jiang HY (2013) Strengthening mechanisms in solution treated Mg–yNd–zZn–xZr alloy. J Mater Sci 48:6367–6376. doi:10.1007/s10853-013-7436-0
16. Li ZM, Luo AA, Wang QG, Peng LM, Fu PH, Wu GH (2013) Effects of grain size and heat treatment on the tensile properties of Mg–3Nd–0.2Zn (wt%) magnesium alloys. Mater Sci Eng A 564:450–460
17. Wang QG (2003) Microstructure effects on the tensile and fracture behavior of aluminum casting alloys A356/357. Metall Mater Trans A 34:2887–2899
18. Li ZM, Fu PH, Peng LM, Wang YX, Jiang HY, Wu GH (2013) Comparison of high cycle fatigue behaviors of Mg–3Nd–0.2Zn–Zr alloy prepared by different casting processes. Mater Sci Eng A 579:170–179
19. Fu PH, Peng LM, Jiang HY, Zhai CQ, Gao X, Nie JF (2007) Zr-containing precipitations in Mg–3 wt%Nd–0.2 wt%Zn–0.4 wt% Zr alloy during solution treatment at 540 °C. Mater Sci Forum 546–549:97–100
20. Bettles CJ, Gibson MA, Zhu SM (2009) Microstructure and mechanical behaviour of an elevated temperature Mg-rare earth based alloy. Mater Sci Eng A 505:6–12
21. Sha G, Zhu HM, Liu JW, Luo CP, Liu ZW, Ringer SP (2012) Hydrogen-induced decomposition of Zr-rich cores in an Mg–6Zn–0.6Zr–0.5Cu alloy. Acta Mater 60:5615–5625
22. Hisa M, Barry JC, Dunlop GL (2002) New type of precipitate in Mg-rare-earth alloys. Phil Magn 82:497–510
23. Basquin OH (1910) The exponential law of endurance tests. Proc ASTM 10:625–630
24. Man J, Obrtlik K, Blochwitz C, Polak J (2002) Atomic force microscopy of surface relief in individual grains of fatigued 316L austenitic stainless steel. Acta Mater 50:3767–3780